

# RESEARCH MEMORANDUM

THROAT -AREA DETERMINATION FOR A CASCADE OF  
DOUBLE -CIRCULAR -ARC BLADES

By Linwood C. Wright and Richard Schwind

Lewis Flight Propulsion Laboratory  
Cleveland, Ohio

NATIONAL ADVISORY COMMITTEE  
FOR AERONAUTICS  
WASHINGTON

November 15, 1955  
Declassified September 17, 1958

NATIONAL ADVISORY COMMITTEE FOR AERONAUTICS

RESEARCH MEMORANDUM

THROAT-AREA DETERMINATION FOR A CASCADE OF DOUBLE-CIRCULAR-ARC BLADES

By Linwood C. Wright and Richard Schwind

SUMMARY

A procedure is derived for approximating the throat area and the choking incidence angle for a compressor geometry wherein the throat area is at the inlet to the cascade of double-circular-arc blades and the leading-edge radius is 0.15 of the maximum thickness. Charts for determining the throat area are presented.

An empirical relation between the choking incidence angle at an inlet relative Mach number of 1.0 and the minimum-loss incidence angle is presented using the available test results for rotor tip, pitch, and hub sections.

INTRODUCTION

Recent advances in compressor performance have been obtained through use of high Mach numbers relative to the rotor blading. At the high Mach numbers, however, the range of blade incidence angles for good performance is reduced, particularly the range of lower values (see ref. 1). Reduced range is associated primarily with a choking of the blade passage at which point the rotor efficiency falls off sharply. It is therefore desirable that no portion of the blade span operate at the choked condition. Consequently, determination of the choking incidence angle is of considerable interest.

In general, the choking incidence angle of a cascade varies with the solidity, blade stagger angle, camber angle, thickness distribution, maximum thickness, Mach number, and some three-dimensional effects. These are the same variables with which the minimum-loss incidence angle also has been observed to vary. These considerations suggest the possibility of obtaining some empirical relation between cascade choking incidence and minimum-loss incidence, perhaps as a function of Mach number.

In order to approximate the cascade choking incidence angle analytically, first it was necessary to determine the cascade throat area.

References 2 and 3 present series of curves from which the throat areas may be found for cascades composed of British C4 base airfoils superimposed on a circular arc and a parabolic camber line, respectively. Throat areas for these cascades were determined graphically and the results correlated empirically. The ratio of the throat area to the inlet area was used to approximate the Mach number effect.

Recently considerable success has been experienced in utilizing double-circular-arc blade sections. Inasmuch as design speed losses and deviation angle (hence, enthalpy rise) are known to vary with incidence angle, it is important to fix the orientation (twist) of each blade to give the optimum possible incidence at all radial sections. Moreover, the necessity for good off-design performance makes knowledge of the low-loss incidence range important to the designer.

The work reported herein presents a reasonably direct procedure for approximating with good accuracy the throat areas for the double-circular-arc sections currently in use. The equations from which the throat area may be found for any given set of design variables are derived in appendix B under the assumption that the throat always occurs at the cascade inlet. The conditions for which this assumption is not fulfilled are indicated. Other limitations to the procedure are also indicated and briefly discussed.

Charts are presented in the form of carpet plots which permit the reader to obtain the throat area directly as a function of the cascade variables with a minimum of linear interpolation. The expression is presented from which the choking incidence angle may be quickly computed once the throat area and inlet relative Mach number are known.

Finally, the available experimental results for circular-arc blade elements are utilized in formulating an approximate relation between the choking incidence angle for an inlet Mach number of 1.0 and the minimum-loss incidence angle.

## ANALYSIS

Compressor-rotor design is generally initiated by determining the inlet- and outlet-velocity diagrams. These diagrams result from the desired or specified thermodynamic and aerodynamic conditions ahead of and behind the rotor along with the rotor rotational speed. From the desired flow turning angle and a prescribed solidity, the necessary blade camber angle is obtained using either experimental cascade data or a prescribed incidence angle and a deviation-angle rule, for example, Carter's rule (ref. 4). For high Mach number designs it is desirable to determine the choking incidence angle so that the design weight flow may be obtained with all sections operating above choking incidence.

In order to determine the choking incidence angle, the blade shape (i.e., for double-circular-arc blades, camber angle, maximum thickness, and leading- and trailing-edge radii), the orientation, and the solidity must be known.

An initial estimate of the incidence and deviation angles will therefore be necessary in order to obtain the blade inlet angle  $\beta_b$  and the camber angle  $\phi$ . (All symbols are defined in appendix A.) The throat area  $d$  may now be found as a function of  $\beta_b$ ,  $\phi$ ,  $t_{\max}$ , and  $\sigma$ . (See fig. 1 for cascade nomenclature.)

### Throat Area

Equations derived in appendix B permit calculation of the throat area for any combination of blade geometrical parameters for which the throat occurs at the blade leading edge. By use of these equations and a leading-edge radius fixed at 0.15 of the maximum blade thickness, the carpet plots (similar to those of ref. 5) were obtained for dimensionless thicknesses of 0.04, 0.08, and 0.12 and are presented in figure 2. From these charts in which all linear dimensions are normalized through division by chord  $c$ , the two-dimensional throat area  $d$  may be obtained as illustrated in the following example. Several readily made interpolations are necessary; however, only the thickness interpolation need be linear.

With the quantities  $\sigma = 1.20$ ,  $t_{\max} = 0.06$ ,  $\phi = 25^\circ$ , and  $\beta_b = 65^\circ$ , the procedure for determining the throat area  $d$  is as follows:

(1) Refer first to figure 2(a) for  $t_{\max} = 0.04$  and select the mat for  $\sigma = 1.00$ .

(2) Locate the point A at the intersection of the lines for  $\beta_b = 65^\circ$  and  $\phi = 25^\circ$ .

(3) In a similar manner, locate the point B on the  $\sigma = 1.50$  mat for the same values of  $\phi$  and  $\beta_b$ .

(4) Pass a curve through the points A and B and parallel to the nearest dotted guide lines.

(5) Using the horizontal scale now for solidity, follow the curve from A toward B a distance corresponding to  $\sigma = 1.20$  (point C).

(6) The value of  $d_{0.04} = 0.431$  read on the vertical scale for point C gives the throat area corresponding to  $t_{\max} = 0.04$ .

(7) Repeat steps (1) to (6) as shown in figure 2(b) to obtain  $d_{0.08} = 0.412$ .

(8) Interpolate linearly between the values for  $t_{\max} = 0.04$  and  $0.08$  to obtain  $d_{0.06} = 0.422$ .

### Choking Incidence Angle

Once the throat area  $d$  is found, the choking incidence may be found from

$$\cos(\beta_b + l_{ch}) = \frac{\sigma d}{\left(\frac{A_{cr}}{A}\right) M_1'} \quad (1)$$

In order to determine the choking incidence angle for an inlet blade relative Mach number of 1.00,  $A_{cr}/A$  is set equal to 1.00, resulting in the expression

$$\cos(\beta_b + l'_{ch}) = \sigma d \quad (1b)$$

### Limitations

The more serious limitations on the accuracy of the procedure for computing the actual compressor choking incidence angle result from (a) the existence of radial components of velocity, (b) nonuniform flow at the cascade throat area, and (c) location of the throat area behind the inlet.

The radial component of velocity leads to a difference in inlet and throat radii and the attendant variation in geometry and blade relative total pressure. Except for extreme cases of hub-radius change (cone half-angles exceeding  $20^\circ$ ), these effects, which in the over-all picture are usually compensating at the hub, will generally have a negligible effect on the pitch and tip. This is particularly true in view of the intended empirical use of these results.

With regard to the throat nonuniformity, a somewhat more elaborate analysis involving the passage mean-line radius at the throat would allow a very close approximation to the effective throat area. Again, however, the empirical character of this work appears to eliminate the necessity for this type of refinement.

For most conventional compressor blades, particularly the tip and pitch sections, the throat will lie at the blade leading edges. The conditions for which this is not true are shown for solidities of 1.50 and 2.00 in figure 3. These curves define the critical points; the region above and to the right of the curves indicates the geometry for which the minimum area is at the inlet. An expression for determination of the critical point results when the slope of the blade pressure surface at the leading edge is equated to the slope of the nearest suction-surface point.

## RESULTS AND DISCUSSION

### Choking Incidence Angle

Preliminary observations indicated that the choking incidence for a blade inlet relative Mach number of 1.0 offered a convenient value for comparative analyses over the range of inlet Mach numbers near 1.0. Under these conditions, choking incidence is a function of blade geometry alone. In the range of rotor relative inlet Mach number of most interest ( $0.80 < M_1 < 1.20$ ), the choking incidence angle at Mach 1.0 will in general differ only slightly from that computed for the actual inlet Mach number. (The throat area  $d$  was found from fig. 1 as described in the ANALYSIS section.) Equation (1b) was used to obtain  $\cos(\beta_b + \iota'_{ch})$  and, hence,  $\iota'_{ch}$ , the choking incidence angle at Mach 1.0.

### Correlation With Minimum-Loss Incidence Angle

As previously noted,  $\iota'_{ch}$  and  $\iota'_m$  depended on the same variables ( $\beta'_b$ ,  $\Phi$ ,  $\sigma$ ,  $t_{max}$ , and  $M_1$ ) when the leading- and trailing-edge radius was fixed as a function of the maximum thickness. Therefore, an attempt was made to obtain an approximate systematic variation between choking incidence angle at Mach 1.0 and the experimentally determined minimum-loss incidence angles for the available transonic rotor results.

Only by separation of the hub, pitch, and tip experimental results could there be obtained any approach to a rational correlation between  $\iota'_{ch}$  and  $\iota'_m$ . In spite of this separation, the hub-section plot of  $\Delta \iota' = (\iota'_m - \iota'_{ch})$  against  $M_1$  (fig. 4(a)) resulted in a broad band of points incapable of supporting an incidence-angle rule. It was observed, however, that for all Mach numbers above 0.60, the minimum-loss incidence angle at the hub always exceeded  $\iota'_{ch}$ . The tip- and pitch-section variation of  $\Delta \iota'$  with inlet relative Mach number might be considered good in view of the very probable and unavoidable experimental error involved in obtaining incidence-angle data. However, to

rotors that have their tips swept down by an appreciable amount, these results must be applied with considerable caution because of the importance of three-dimensional effects.

In figure 4(b), data from eight separate rotor pitch sections and a two-dimensional cascade are shown to result in values for  $\Delta l'$  against  $M_1$  which, except for a few stray points, lie in a reasonably narrow band. Somewhat less scatter is observed for the bulk of the tip-section data (fig. 4(c)). This narrow band at the tip is of particular interest, of course, inasmuch as the highest Mach numbers exist at the tip leading to the minimum range of low-loss incidence. Conversely, some tolerance may be allowed at the pitch and hub where the Mach numbers are lower and the range of low-loss incidence is somewhat greater. For the inverse procedure, a minimum-loss incidence angle may be found through a short iterative process by utilizing the curves of figure 4 and a deviation-angle rule such as Carter's rule (fig. 5).

#### CONCLUDING REMARKS

A procedure is derived for approximating the throat area and the choking incidence angle for a cascade of double-circular-arc blades with the throat at the inlet and a leading-edge radius of 0.15 of the maximum thickness. Charts for determining throat area are presented.

An empirical relation between the choking incidence angle at an inlet relative Mach number of 1.0 and the minimum-loss incidence angle is presented using the available rotor-tip, pitch, and hub-section test results.

Lewis Flight Propulsion Laboratory  
National Advisory Committee for Aeronautics  
Cleveland, Ohio, August, 29, 1955

## APPENDIX A

## SYMBOLS

The following symbols are used in this report:

$A_{cr}/A$	ratio of critical area (sonic flow) to actual flow area at any point in flow
$c$	blade chord
$D, E, F$	coefficients defined by eq. (A2)
$d$	cascade throat area per unit blade span (throat height is normalized through division by blade chord)
$\lambda$	incidence angle defined as angle between flow direction and tangent to blade mean line at leading edge
$\lambda'_{ch}$	choking incidence angle defined as angle between leading-edge flow direction for choked blade passage and blade mean line tangent at inlet
$\lambda'_{ch}$	$\lambda'_{ch}$ for inlet relative Mach number of 1.0
$\Delta\lambda'$	$\lambda'_m - \lambda'_{ch}$
$M$	Mach number
$m$	coefficient defined in fig. 5
$R$	radius of blade mean line (see appendix B)
$r$	blade leading-edge radius (normalized through division by chord)
$s$	blade spacing
$t_{max}$	maximum blade thickness (normalized through division by chord)
$\beta_b$	blade inlet angle defined as angle between line tangent to blade mean line at leading edge and axial direction
$\beta_f$	flow direction defined as angle between flow direction and axial direction



- $\gamma$   $\beta_b - \frac{\phi}{2}$  (see fig. 1)
- $\delta$  deviation angle
- $\eta, \xi$  points on coordinate system (fig. 1) defined by eqs. (A3) and (A4)
- $\lambda$  Lagrange's multiplier defined by eq. (A11)
- $\sigma$  blade solidity,  $c/s$
- $\phi$  camber angle defined as angle between tangent to blade mean line at inlet and exit

## Subscripts:

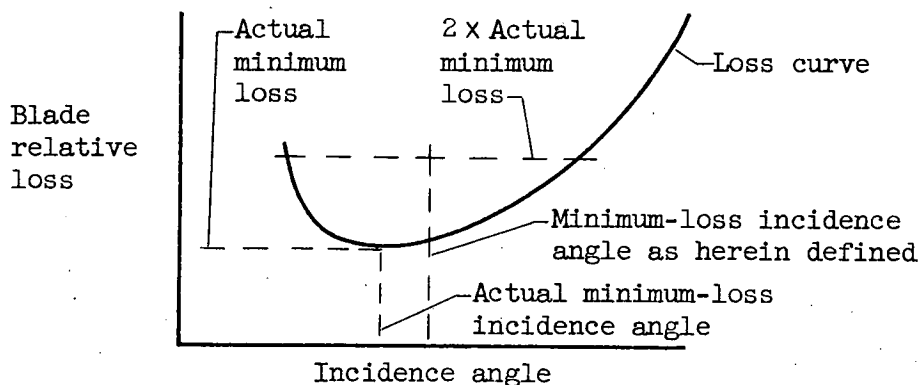
m minimum loss

l inlet rotor

## Superscript:

' relative to rotor blade row

For current purposes, the minimum-loss incidence will be defined (see sketch) as the midpoint of the horizontal line intersecting the two branches of the curve of loss against incidence angle at loss values double the lowest loss points.



While this particular definition is more or less arbitrary and will not generally locate the actual minimum-loss incidence point, the following considerations indicate its usefulness. Usually any particular blade row will be required to operate over a range of weight flows at fixed speeds and, hence, at a range of incidence angles on both sides of the design value. In many instances, therefore, it will be preferable to locate the design operating point of a blade row at the midpoint of the low-loss range rather than at the absolute minimum-loss incidence point.

## APPENDIX B

## DERIVATION OF CASCADE THROAT AREA

A reasonably direct derivation of the cascade minimum throat width (area for unit span) may be obtained as follows. The equation of the circle whose arc makes up the blade mean line in figure 1 may be written as

$$x^2 + y^2 + 2yR = 0 \quad (A1)$$

where all linear dimensions are normalized through division by the chord  $c$ . The radius  $R$  is therefore given as

$$R = \frac{1}{2 \sin \frac{\Phi}{2}}$$

The general equation of a circle will be used to represent the pressure and suction surfaces:

$$x^2 + y^2 + Dx + Ey + F = 0 \quad (A2)$$

From the symmetry of the blade surfaces about the  $y$ -axis, the coefficient  $D = 0$ . Only the coefficients  $E$  and  $F$  in the general equation (2) need be evaluated. The asymmetrical points on the arcs are used for evaluating these constants.

From figure 1, the coordinates of suction surface point  $g$  are

$$\left. \begin{aligned} x_g &= -\frac{1}{2} - r \sin \frac{\Phi}{2} = -\left(\frac{1}{2} + r \sin \frac{\Phi}{2}\right) = -\xi \\ y_g &= -\left(\frac{1}{2} \tan \frac{\Phi}{4} - r \cos \frac{\Phi}{2}\right) = -\eta \end{aligned} \right\} \quad (A3)$$

From symmetry, the coordinates of  $f$  are

$$\left. \begin{aligned} x_f &= \frac{1}{2} + r \sin \frac{\Phi}{2} = \xi \\ y_f &= -\left(\frac{1}{2} \tan \frac{\Phi}{4} - r \cos \frac{\Phi}{2}\right) = -\eta \end{aligned} \right\} \quad (A4)$$

Coordinates of the point e are

$$\left. \begin{aligned} x_e &= 0 \\ y_e &= \frac{t_{\max}}{2} \end{aligned} \right\} \quad (A5)$$

Substitution of the coordinates of the points e and f into equation (2) with  $D = 0$  leads to the following values for the coefficients E and F:

$$E = \frac{\xi^2 + \eta^2 - \frac{t_{\max}^2}{4}}{\eta + \frac{t_{\max}}{2}} \quad (A6)$$

$$F = -\xi^2 - \eta^2 + \eta \left( \frac{\xi^2 + \eta^2 - \frac{t_{\max}^2}{4}}{\eta + \frac{t_{\max}}{2}} \right) \quad (A7)$$

The distance  $d$  (fig. 1) is given in general by

$$d = \sqrt{(x - x_0)^2 + (y - y_0)^2} \quad (A8)$$

where  $x_0$  and  $y_0$ , the coordinates of the point a', (upper terminus of  $d$ ) are given very closely as

$$\left. \begin{aligned} x_0 &= -\frac{1}{2} + \frac{1}{\sigma} \sin \gamma + r \sin \frac{\Phi}{2} \\ y_0 &= -\frac{1}{2} \tan \frac{\Phi}{4} - r \cos \frac{\Phi}{2} + \frac{\cos \gamma}{\sigma} \end{aligned} \right\} \quad (A9)$$

where  $\gamma = \beta_b - \frac{\Phi}{2}$ .

Now  $d$ , or more conveniently,  $d^2$ , must be minimized subject to the condition that the point  $x, y$  lies on the suction line (or surface for unit span)  $d_{sef}$  given by

$$x^2 + y^2 + Ey + F = 0 \quad (A10)$$

A convenient procedure (ref. 6) utilizes Lagrange's multipliers as follows: Equations (A8) and (A10) may be combined with the multiplier to form the function

$$G = (x - x_0)^2 + (y - y_0)^2 - \lambda(x^2 + y^2 + Ey + F) = 0 \quad (\text{A11})$$

where  $\lambda$  is a multiplier.

The function  $G$  may now be differentiated in turn with respect to  $x$  and  $y$  yielding

$$\frac{\partial G}{\partial x} = 2(x - x_0) - 2\lambda x = 0 \quad (\text{A12})$$

and

$$\frac{\partial G}{\partial y} = 2(y - y_0) - \lambda(2y + E) = 0 \quad (\text{A13})$$

Equations (A10), (A12), and (A13) may be solved simultaneously for  $x$ ,  $y$ , and  $\lambda$  defining the point  $h$  (fig. 1) on the suction surface nearest  $a'$ . (Extremals other than minimums are eliminated, from geometrical considerations.) From equation (A12),

$$\lambda = 1 - \frac{x_0}{x} \quad (\text{A14})$$

Substitution of  $\lambda$  in equation (A13) yields

$$y = \frac{x}{x_0} y_0 + \frac{E}{2} \frac{x}{x_0} - \frac{E}{2} \quad (\text{A15})$$

Use of equation (A15) for  $y$  in equation (A10) leads to

$$\frac{x}{x_0} = \left( \frac{\frac{E^2}{4} - F}{x_0^2 + y_0^2 + Ey_0 + \frac{E^2}{4}} \right)^{\frac{1}{2}} \quad (\text{A16})$$

Finally, equations (A15) and (A16) combine to yield

$$y = \left( y_0 + \frac{E}{2} \right) \left( \frac{\frac{E^2}{4} - F}{x_0^2 + y_0^2 + Ey_0 + \frac{E^2}{4}} \right)^{\frac{1}{2}} - \frac{E}{2} \quad (\text{A17})$$

Thus, the throat area  $d$  may be found from the solution of the preceding equations in the following order:

- (a) Solve equation (A9) for  $x_0$  and  $y_0$
- (b) Obtain  $\xi$  and  $\eta$  from equation (A3)
- (c) Obtain the coefficient  $E$  from equation (A6)
- (d) Solve equation (A7) for  $F$
- (e) Solve equation (A16) for  $x/x_0$  and  $x$
- (f) Solve equation (A17) for  $y$
- (g) Obtain distance  $d$  from equation (A8)

#### REFERENCES

1. Andrews, S. J.: Tests Related to the Effect of Profile Shape and Camber Line on Compressor Cascade Performance. Rep. No. R.60, British N.G.T.E., Oct. 1949.
2. Carter, A. D. S.: Throat Areas of Compressor Blade Cascades Derived for the Base Aerofoil C.4. Power Jets Memo. No. M.1025, Power Jets, Ltd., Oct. 1944.
3. Hughes, Hazel P.: Throat Areas for the Parabolic Arc Cambered Aerofoil C.4 in Cascade. Memo. No. M.157, British N.G.T.E., Aug. 1952.
4. Carter, A. D. S.: The Low Speed Performance of Related Airfoils in Cascade. Rep. No. R. 55, British N.G.T.E., Sept. 1949.
5. Felix, A. Richard: Summary of 65-Series Compressor-Blade Low-Speed Cascade Data by the Use of the Carpet-Plotting Technique. NACA RM L54H18a, 1954.
6. Franklin, Philip: Methods of Advanced Calculus. McGraw-Hill Book Co., Inc., 1944, pp. 67-68

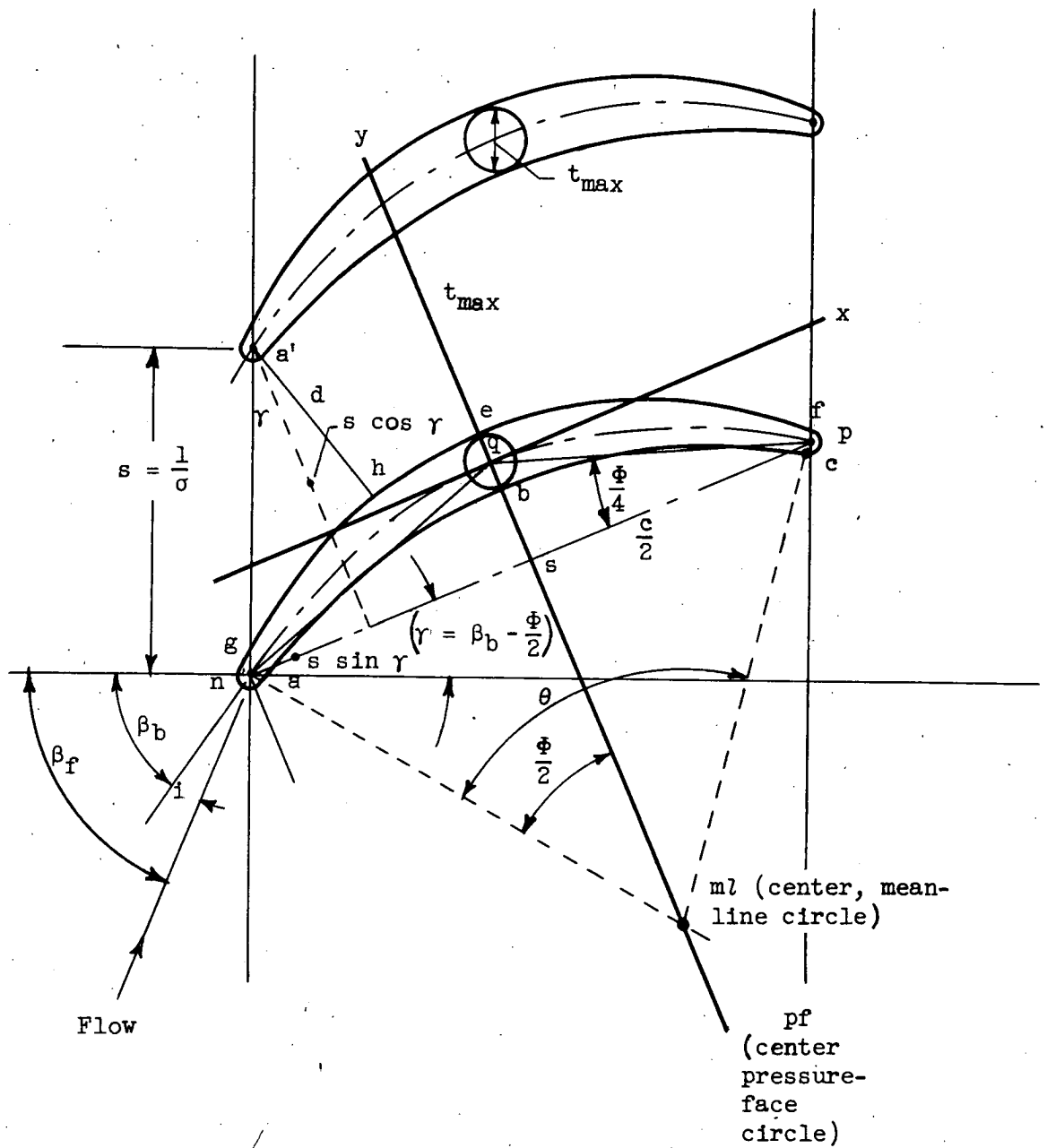
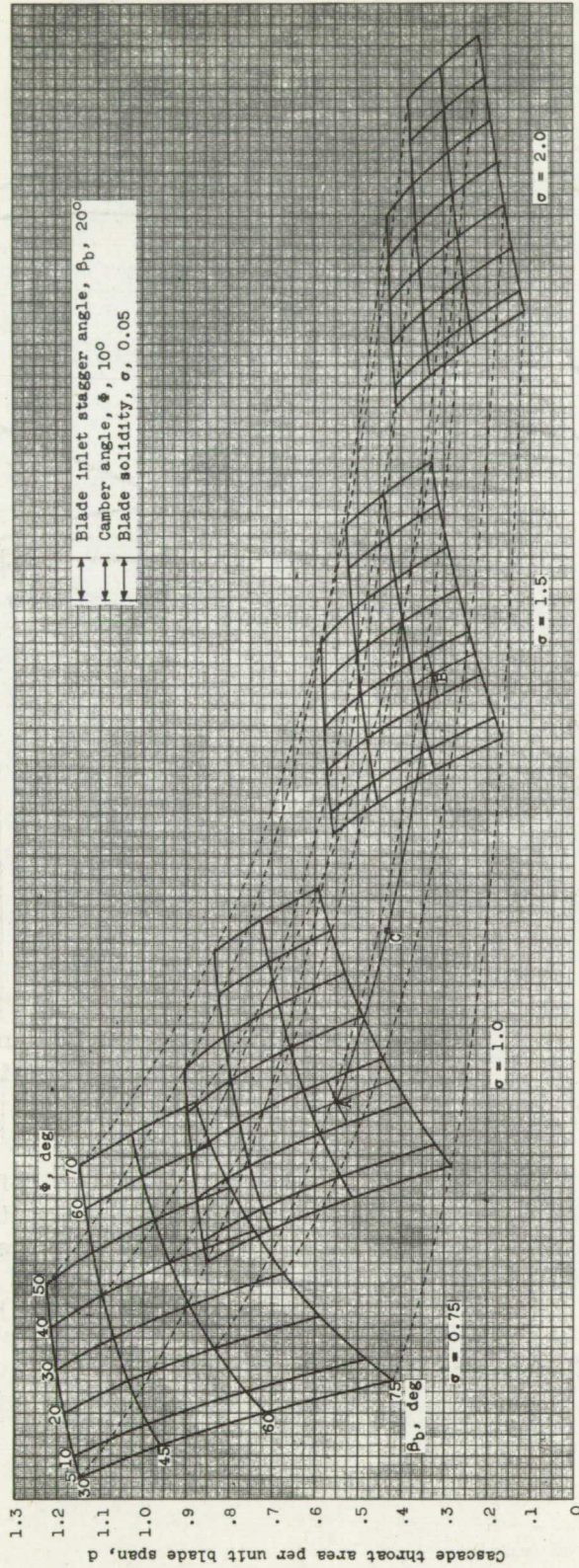


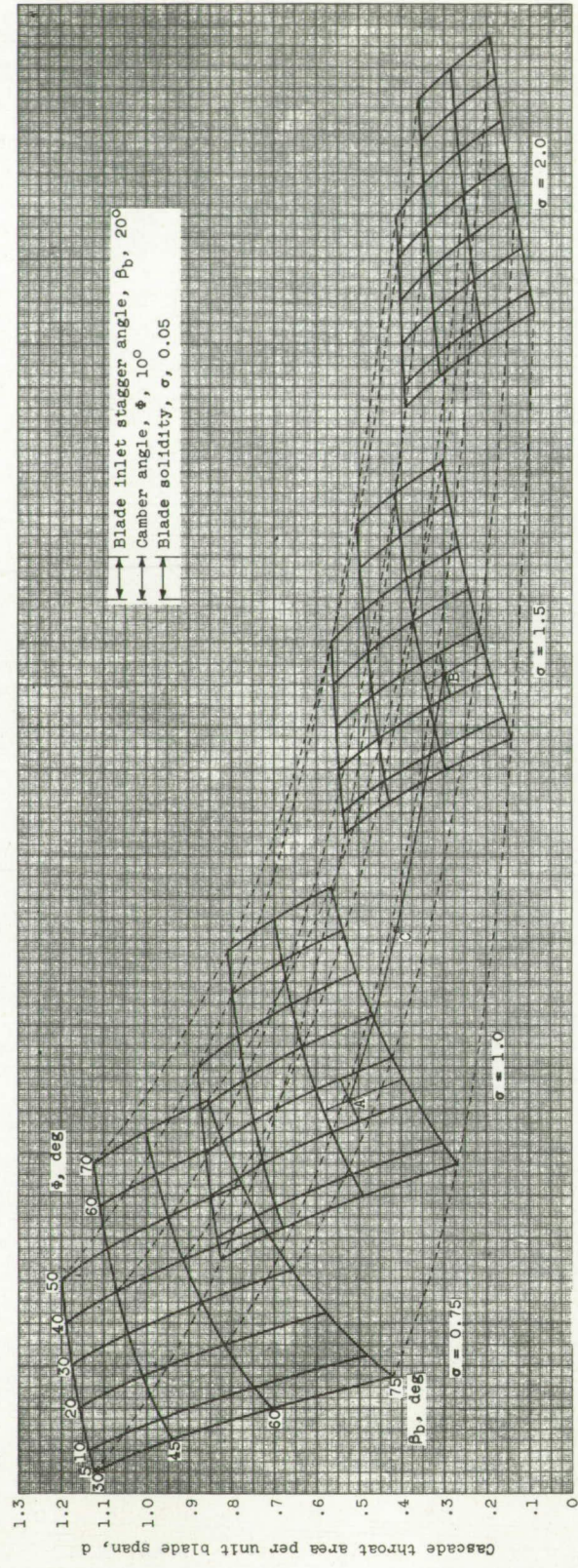
Figure 1. - Cascade notation.



(a) Maximum blade thickness, 0.04.

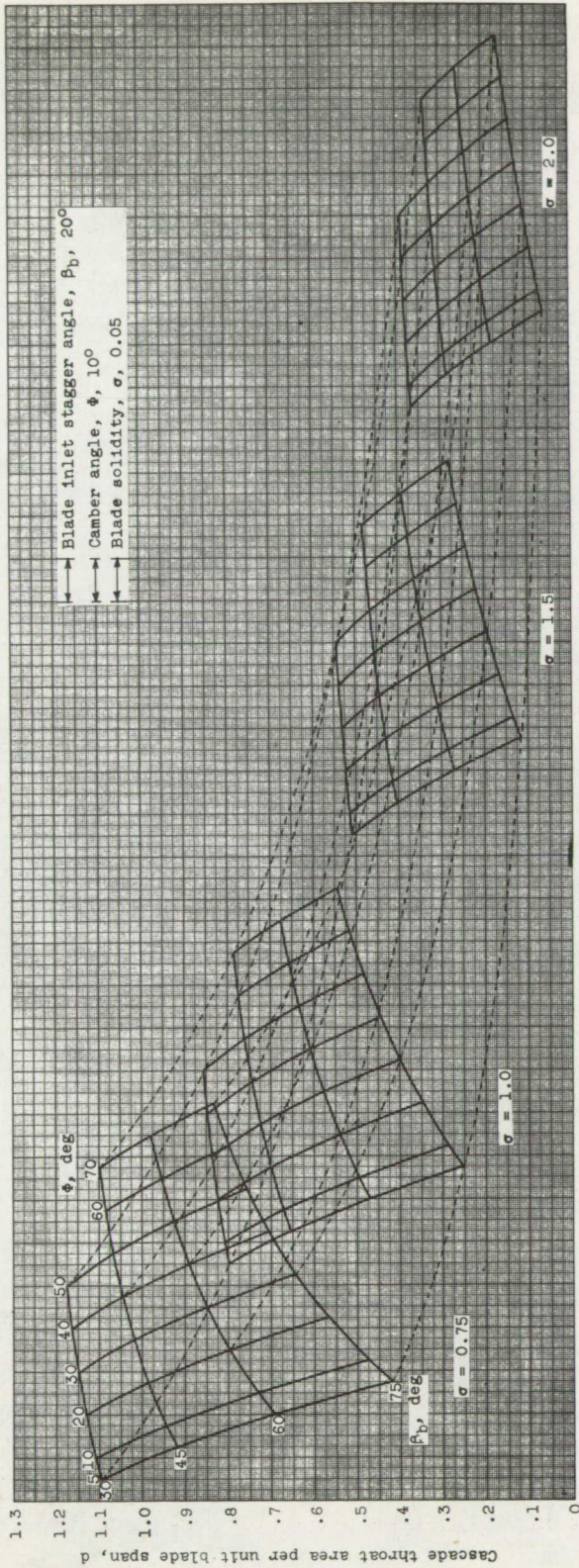
Figure 2. - Throat-area variation with cascade geometry. (A large working copy of this figure may be obtained by using the request card bound in the back of the report.)





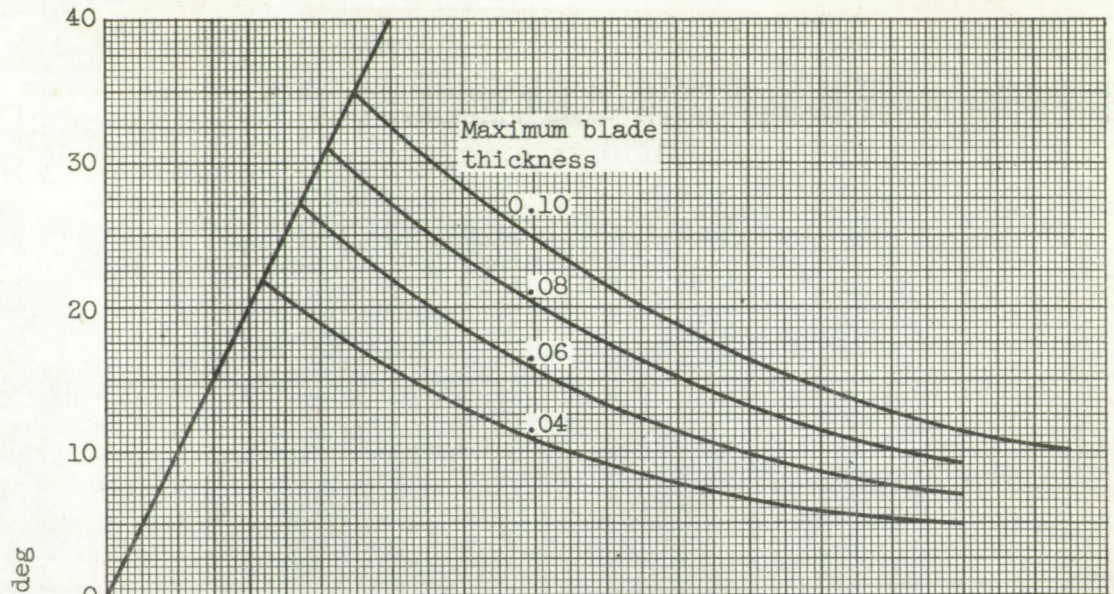
(b) Maximum blade thickness, 0.08.

Figure 2. - Continued. Throat-area variation with cascade geometry. (A large working copy of this figure may be obtained by using the request card bound in the back of the report.)

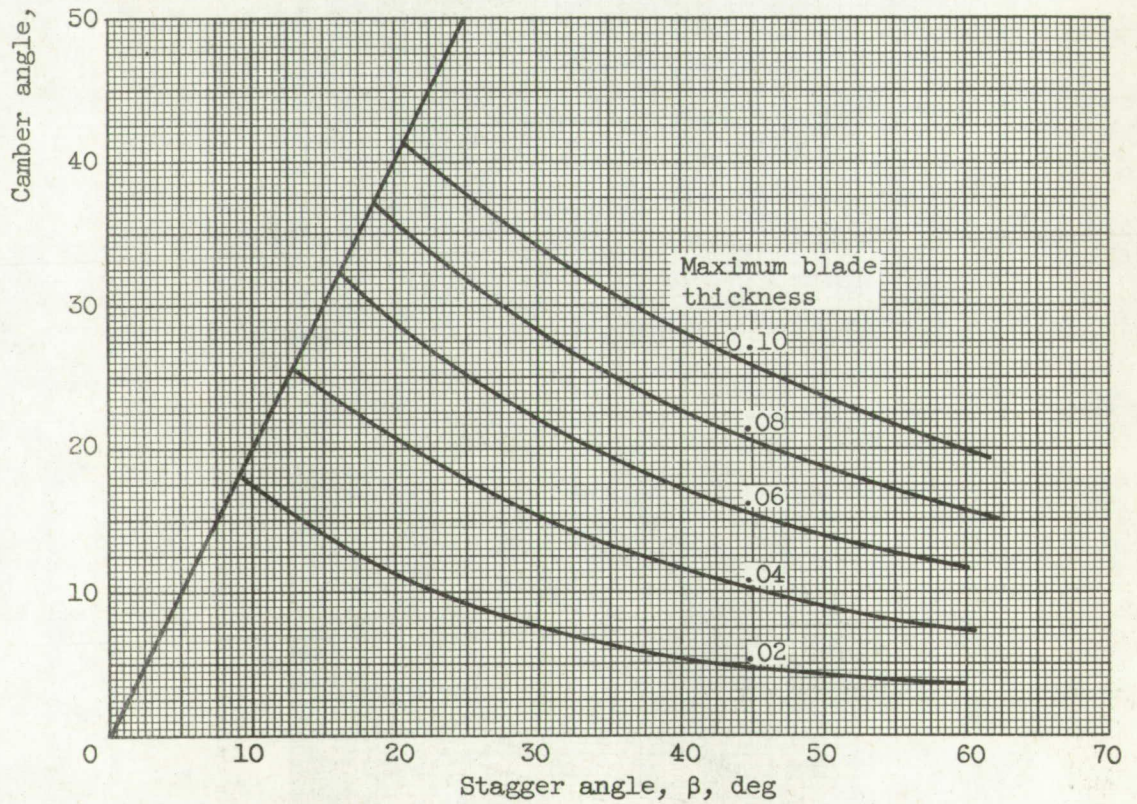


(c) Maximum blade thickness, 0.12.

Figure 2. - Concluded. Throat-area variation with cascade geometry. (A large working copy of this figure may be obtained by using the request card bound in the back of the report.)

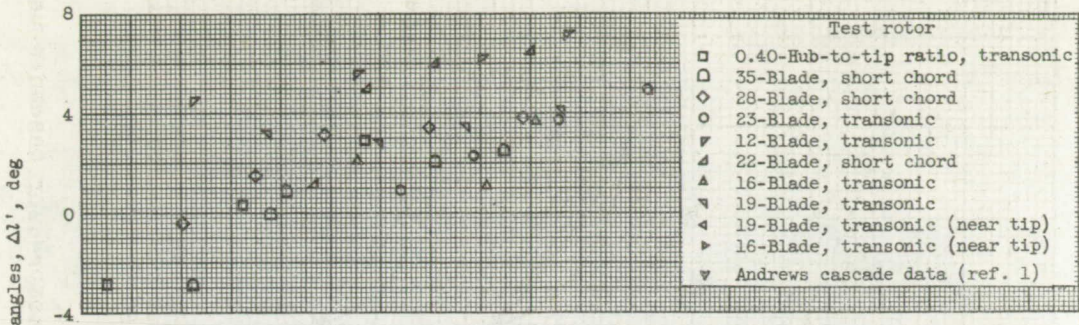


(a) Blade solidity, 1.50.

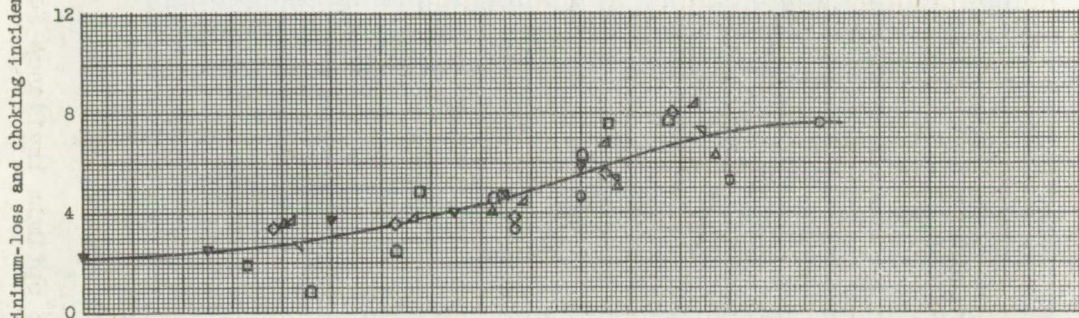


(b) Blade solidity, 2.0.

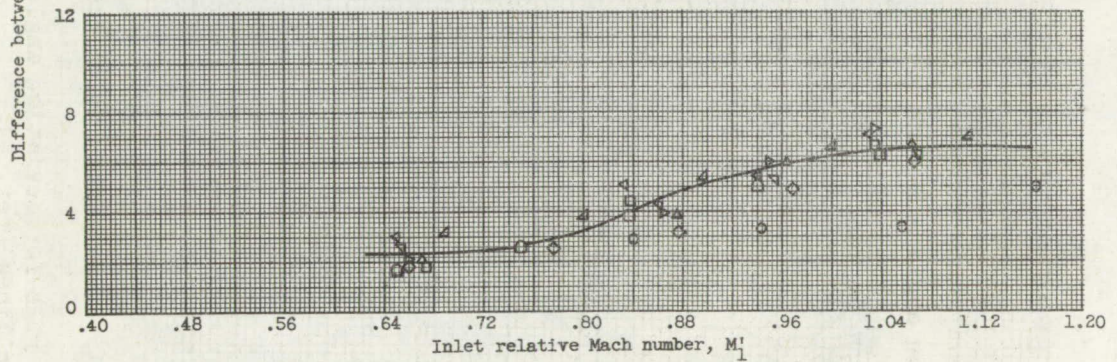
Figure 3. - Limiting conditions for minimum area at leading edge.



(a) Section near hub.



(b) Pitch section.



(c) Section near tip.

Figure 4. - Variation of minimum-loss incidence angle with choking incidence angle at Mach 1.0 for double-circular-arc rotor blade sections.

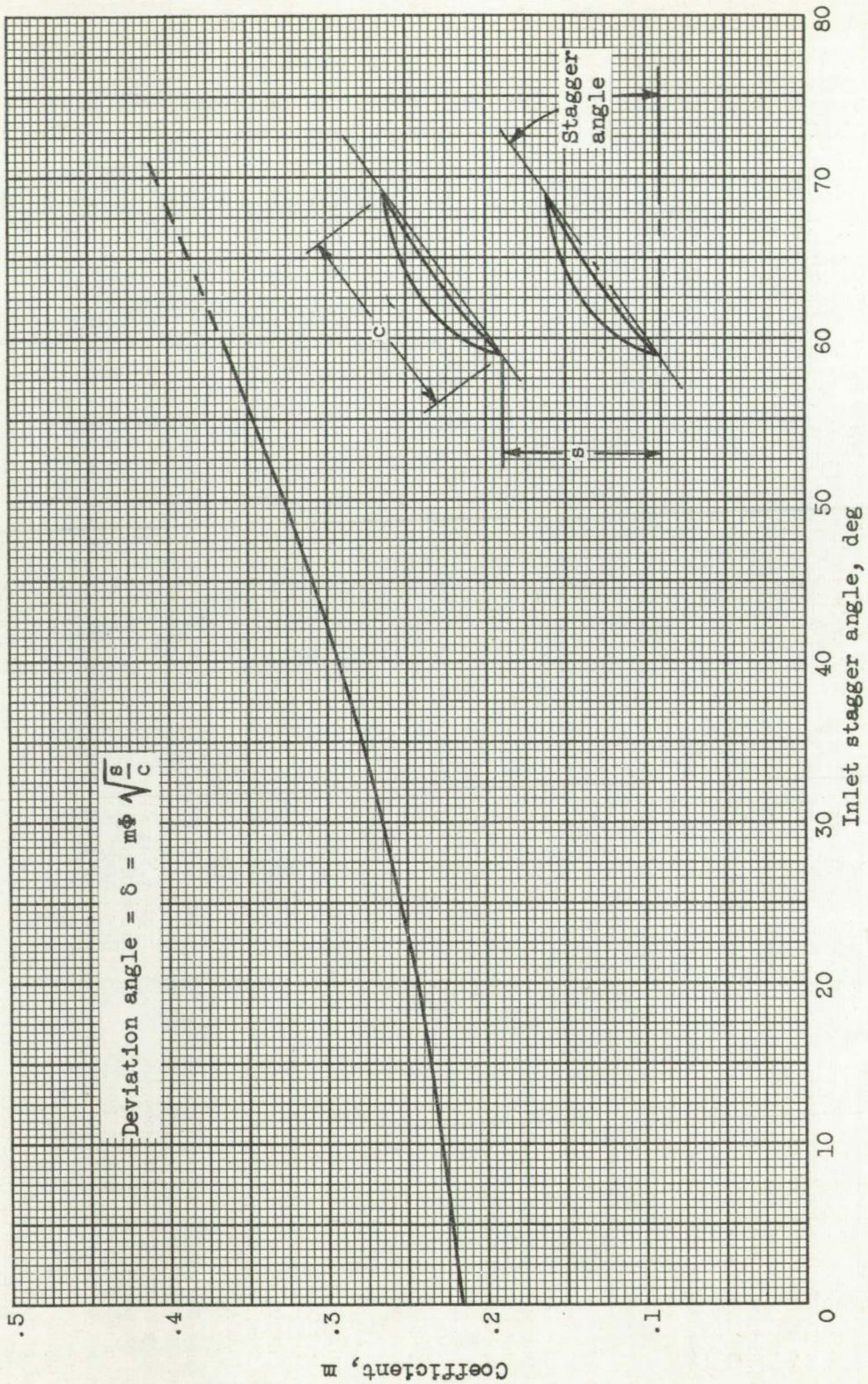


Figure 5. - Carter's rule for deviation angle at optimum incidence for compressor cascades using circular-arc camber lines (ref. 4).